Systems & Control Transactions

Original Research Article
Peer Reviewed Conference Proceeding
ESCAPE 36 - European Symposium on Computer Aided Process Engineering
Sheffield, UK. 21-24 June 2026

PSE PRESS

Multi-Objective Optimisation of Pressure Swing Adsorption Systems via Symbolic Regression

Carine Menezes REBELLO[a*], Amilton Barbosa BOTELHO JUNIOR[a], Anderson Rapello DOS SANTOS[bc], and Idelfonso B. R. NOGUEIRA[a]

[a] Department of Chemical Engineering, Norwegian University of Science and Technology, Trondheim, Norway
[b] Petroleo Brasileiro S.A. (PETROBRAS), Wells/Well Engineering, Brazil.
[c] Pontifical Catholic University of Rio de Janeiro (PUC-Rio), Department of Mechanical Engineering (DEM), Rio de Janeiro, RJ, Brazil.
* Corresponding Author: carine.m.rebello@ntnu.no.

ABSTRACT

This work explores symbolic regression (SR) as an interpretable surrogate modelling approach for the multi-objective optimisation of pressure swing adsorption (PSA) systems for CO_2 capture. A first-principle model was used as a virtual plant to generate synthetic datasets covering the operating space defined by cycle step durations. Two surrogate frameworks were developed and compared: SR models derived through evolutionary search and deep neural networks (DNNs) trained via Hyperband-based tuning. Both surrogates were used as simulation models within an optimisation procedure based on a particle swarm optimisation (PSO) algorithm to maximise CO_2 purity and recovery. While DNNs achieved the lowest prediction errors (MSE ≈ $10^{-6)}$, the SR surrogates provided compact analytical representations and significantly faster optimisation. The SR framework yielded a denser and more diverse Pareto front (4345 vs 508 points). It was about 34 times faster (38.6 s vs 1331 s), confirming its efficiency for surrogate-based optimisation of cyclic adsorption processes.

Keywords: PSA, multi-objective optimisation, surrogate models, optimality, symbolic regression

INTRODUCTION

Pressure swing adsorption (PSA) systems play a key role in gas separation technologies due to their flexibility, high efficiency, and low maintenance costs (Capra et al., 2018; Habib et al., 2016). They have been extensively employed in processes ranging from air separation (Kamin et al., 2022; Tian et al., 2022) and hydrogen purification (Luberti and Ahn, 2022; Kalman et al., 2022) to carbon dioxide (CO_2) capture from flue gases (Nikolaidis et al., 2016, 2015). Despite their industrial maturity, optimisation of PSA units remains challenging due to their inherently cyclic operation, strong multiscale dynamics, and the tight coupling between adsorption, desorption, and switching phases, which lead to highly nonlinear and constrained process behaviour (Khajuria & Pistikopoulos, 2013; Leperi et al., 2019). The coupled mass, heat, and momentum balances that govern adsorption and desorption transitions must be solved repeatedly over multiple cycles until the system reaches a cyclic steady state (CSS), resulting in a computationally expensive optimisation problem governed by large sets of stiff partial differential equations (PDEs) (Ward and Pini, 2022; Rebello & Nogueira, 2024).

Surrogate modelling techniques have emerged as an alternative to accelerate process optimisation while retaining sufficient physical accuracy. Surrogate-based optimisation replaces the high-fidelity first-principles model with an approximate data-driven representation that captures the input-output relationships between decision variables (e.g., step durations, pressures, and reflux ratios) and process performance metrics (e.g., CO_2 purity and recovery).

These surrogate models have been successfully applied to PSA, generating Pareto fronts that describe the trade-offs between competing objectives, such as purity, recovery, and energy consumption (De Witte et al., 2021; Panerati et al., 2019; Zhang et al., 2022).

Among the various surrogate modelling strategies, deep neural networks (DNNs) have received particular attention (Costa et al., 2024; Nogueira et al., 2022; Subraveti et al., 2019). As demonstrated by Rebello and

Nogueira (2024), DNN-based surrogate frameworks can reliably approximate the nonlinear behaviour of cyclic adsorption systems, drastically reducing simulation time and enabling systematic multi-objective optimisation. The resulting operating maps help identify optimal process configurations and inform decision-making. Despite their predictive accuracy, these data-driven models remain largely opaque, offering limited interpretability and little insight into the physical or phenomenological mechanisms underlying adsorption dynamics (Rebello et al., 2024).

To overcome these limitations, recent research has begun to explore more transparent machine learning paradigms, in which the emphasis shifts from pure prediction to computational efficiency and analytical tractability. In this context, SR offers a promising approach (Makke & Chawla, 2024; Quade et al., 2016; Angelis et al., 2023). Unlike neural networks, which encode relationships implicitly through parameters distributed in hidden layers, SR explicitly searches for analytical expressions that best fit the available data (Rebello et al., 2024; Hu & Zhang, 2023). By combining evolutionary search and sparse regression principles, symbolic regression identifies compact, readable equations that capture system behaviour while revealing underlying physical trends and nonlinear dependencies.

Symbolic regression has been increasingly adopted across a wide range of engineering applications. In process monitoring and fault detection, SR has been used to derive interpretable diagnostic expressions directly from process data (Hale et al., 2022). In soft sensing, SR has been applied to construct explicit input-output mappings for inferential estimation of difficult-to-measure variables (Kay et al., 2024). In the context of control, SR has been employed to identify compact symbolic controllers and model predictive control surrogates that are both computationally lightweight and physically transparent (Scheffold et al., 2021). For optimisation, SR-derived surrogates have been embedded into mathematical programming frameworks to enable gradient-based search and reduce evaluation cost (Sofronova et al., 2021). More broadly, SR has demonstrated strong potential for scientific discovery, recovering governing equations from data across physics, chemistry, and materials science (Angelis et al., 2023).

Beyond its direct application as a surrogate modelling tool, SR offers several promising extensions, particularly relevant to computationally intensive multi-objective optimisation problems. The analytical nature of SR expressions enables direct embedding into algebraic optimisation solvers, avoiding the matrix operations and numerical differentiation overhead inherent to black-box models such as DNNs, which becomes especially advantageous when objective function evaluations must be performed repeatedly across large swarms or populations (Cozad et al., 2014). Furthermore, SR-derived surrogates naturally produce smooth, differentiable expressions that facilitate gradient-based search and yield denser, more diverse Pareto fronts at a lower computational cost, while also producing a significantly richer set of optimal solutions. These properties suggest that SR could be extended to higher-dimensional multi-objective problems, to online re-optimisation under changing operating conditions, and to real-time decision support in CO_2 capture systems, where computational efficiency is a critical practical constraint.

However, symbolic regression models have not yet been investigated for PSA systems. This represents a notable gap in the emerging literature on machine learning applications in chemical process systems, where the potential of faster surrogate models remains largely unexplored. Moreover, given the highly nonlinear nature of PSA dynamics, the behaviour of SR-based surrogates requires careful assessment, as these models may introduce spurious or artificial local minima in the optimisation landscape if not properly regularised and validated.

In this context, the objective of this work is to compare the performance of DNN and SR surrogate models for the optimisation of PSA systems, and to evaluate whether SR-based models can effectively serve as reliable and computationally efficient surrogates, where interpretability is understood as a consequence of the analytical nature of SR expressions rather than a claim of physical correspondence to adsorption dynamics.

METHODOLOGY

The overall methodology adopted in this study is illustrated in Figure 1. The methodology is structured into four main stages: data curation (Section 2.1), SR model (Section 2.2), DNN model (Section 2.3), and multi-objective optimisation (Section 2.4).

The case study investigated in this work concerns the optimisation of a single-column PSA unit for capturing CO_2 from a binary CO_2/N_2 mixture. The PSA process operates cyclically, relying on the preferential adsorption of CO_2 over N_2 onto a solid adsorbent, zeolite 13X, under alternating pressure conditions. Each cycle comprises a sequence of steps (Figure 2): pressurisation (pres), adsorption (ads), heavy reflux (HR), depressurisation (depress) and light reflux (LR). During the pressurisation stage, the column pressure is increased to the adsorption level; in the adsorption step, CO_2 is selectively retained by the zeolite, while N_2 exits as the light product. The subsequent depressurisation and purge steps promote CO_2 desorption and restore the adsorbent's capacity for the next cycle. The process is governed by key decision variables, including the durations of each step (t_{pres}, t_{ads}, t_{depres}, and t_{purge}). The leading performance indicators considered are CO_2 purity and CO_2 recovery, which depend nonlinearly on these operational conditions and on the

thermodynamic and kinetic properties of the zeolite 13X adsorbent.

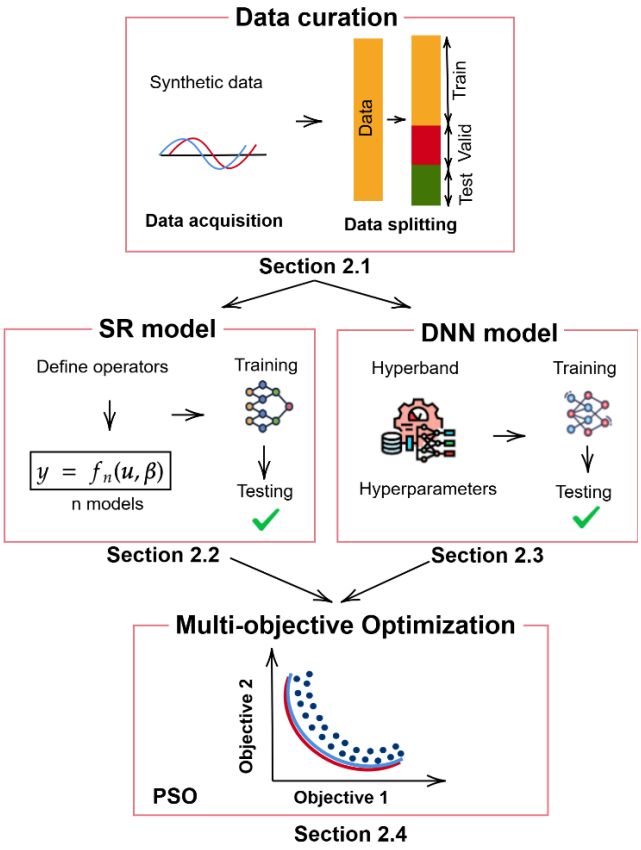

Figure 1. Diagram describing the methodology adopted in this work.

The detailed formulation of the mechanistic PSA model used in this work, including the PDE system, modelling assumptions, boundary and initial conditions, and the adopted kinetic and process parameters, is presented in Rebello and Nogueira (2024).

Data curation

Synthetic data were generated using a mechanistic PSA model implemented as a virtual plant. The sampling of operating conditions was performed using Latin Hypercube Sampling (LHS) to ensure a uniform and statistically independent exploration of the design space. The selected input variables correspond to the step durations of the PSA cycle, pressurisation (t_{pres}), adsorption (tads), heavy reflux (t_{HR}), depressurisation (t_{depres}), and light reflux (t_{LR}), which were systematically varied within physically feasible limits. For each LHS sample, the virtual plant was simulated until a cyclic steady state (CSS) was reached, and the corresponding process performance indicators were recorded. The model outputs, or target variables, are CO_2 purity and recovery, which quantify the PSA process's separation efficiency and product quality.

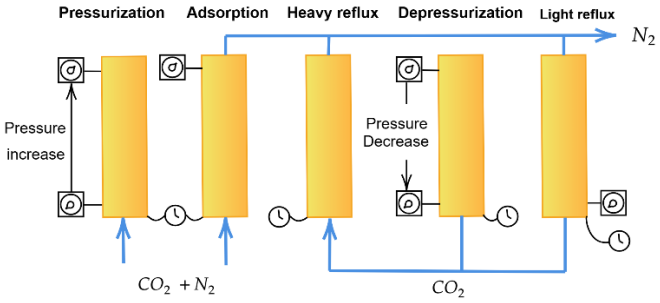

Figure 2. Schematic representation of the PSA cycle for CO_2 capture from a CO_2/N_2 gas mixture, illustrating the successive steps.

The complete dataset was then curated to remove incomplete or non-convergent simulations and subsequently normalised to improve numerical stability during model training. Finally, the curated data were randomly split into training (70 %), validation (15 %), and testing (15 %) subsets. This partition ensures that the surrogate models, both SR and DNN, are trained on representative data while preserving independent sets for unbiased performance evaluation and generalisation assessment.

SR model

The SR framework was employed to identify analytical surrogate models that capture the nonlinear relationship between the PSA operating variables and the process performance indicators, namely CO_2 purity and CO_2 recovery. Symbolic regression formulates this task as a nonlinear regression problem of the form:

$$\boldsymbol{y} = \boldsymbol{f}(\boldsymbol{u_n}, \boldsymbol{\beta}) \quad (1)$$

where u denotes the vector of decision variables (step durations), and β represents the fitted parameters. Candidate expressions are iteratively constructed by combining elementary mathematical operators: {+, −, ×, ÷, sin, cos, exp, log} and constants through an evolutionary symbolic search. This process explores a large function space while progressively selecting the most representative equations based on their predictive accuracy and structural simplicity.

Model selection was guided by a multi-objective fitness criterion that balances prediction error, quantified by the mean squared error (MSE) on the validation dataset, with a complexity penalty proportional to expression length.

The evolutionary search was terminated once convergence was achieved, i.e., when no significant improvement in model accuracy or parsimony was observed.

The best-performing symbolic expressions for CO_2 purity and recovery were then independently validated using the testing subset. These analytical surrogates

replace the high-fidelity PSA model in the multi-objective optimisation framework.

The SR models were developed in Python using the PySRRegressor package (Tonda, 2025) (see: https://astroautomata.com/PySR/), an open-source library for SR that combines genetic programming with simulated annealing for evolutionary search. The algorithm was run with random initialisation, and multiple repetitions were performed to ensure convergence to consistent solutions.

DNN model

The same dataset generated by the mechanistic PSA model was also used to identify the DNN models. The network architecture was defined using the HYPERBAND algorithm (Li et al., 2018) (see: https://keras.io/keras_tuner/api/tuners/hyperband/), which efficiently explores the hyperparameter space to identify near-optimal configurations. The DNNs adopted a multiple-input single-output (MISO) structure, where the input layer receives the PSA decision variables t_{pres}, t_{ads}, t_{HR}, t_{depres}, and t_{LR}, and the output layer provides a single process indicator, either CO_2 purity or CO_2 recovery.

The search space considered the number of hidden layers (ranging from 1 to 5), the number of neurons per layer (from 50 to 300 in steps of 50), activation functions (ReLU and tanh), and learning rates (0.0001, 0.001, and 0.01). Each candidate model was trained using the MSE as the loss function, with the Adam optimiser configured according to the selected learning rate.

Model training aimed to minimise the MSE between predicted and target values, while the mean absolute error (MAE) was also monitored as an auxiliary metric. Each model was trained for up to 1000 epochs, with early stopping and dropout regularisation applied to prevent overfitting and improve generalisation.

After training, the resulting DNN models were validated on the independent test set to assess predictive accuracy. The best-performing networks were subsequently integrated into the multi-objective optimisation framework.

Multi-objective optimisation

The optimisation stage aims to identify the operating conditions that maximise CO_2 purity and recovery, as predicted by the surrogate models. The problem is formulated as a multi-objective optimisation (MOO) task, in which both objectives are maximised simultaneously subject to operational constraints. Mathematically, it can be expressed as:

$$\begin{cases} \max Pur_{CO_2}(\boldsymbol{u}, \boldsymbol{\beta}) \\ \max Rec_{CO_2}(\boldsymbol{u}, \boldsymbol{\beta}) \end{cases} \tag{2}$$

subject to:

$$\boldsymbol{u} \in [\boldsymbol{u_{min}}, \boldsymbol{u_{max}}] \tag{3}$$

where **u** represents the decision variable vector containing the step durations of the PSA cycle, and β denotes the surrogate model parameters. The objective functions are defined as follows:

$$Pur_{CO_2} = \frac{moles_{CO_2,out}\big|_{depress} + moles_{CO_2,out}\big|_{LR}}{moles_{CO_2,total}\big|_{depress} + moles_{CO_2,total}\big|_{LR}} \tag{4}$$

$$Rec_{CO_2} = 1 - \frac{moles_{CO_2,out}\big|_{ads}}{moles_{CO_2,in}\big|_{press} + moles_{CO_2,in}\big|_{ads}} \tag{5}$$

The multi-objective problem was solved using the particle swarm optimisation (PSO) algorithm, chosen for its efficiency in handling nonlinear and nonconvex search spaces. Each surrogate model, SR, and deep neural network, DNN, was embedded within the optimisation routine to compute the objective functions at each iteration. The algorithm simultaneously explores the trade-off between CO_2 purity and recovery, producing a Pareto front that reflects the optimal balance between these competing objectives. This formulation enables a direct comparison of the optimisation performance obtained with SR- and DNN-based surrogates in terms of accuracy, smoothness, and convergence behaviour.

RESULTS AND DISCUSSIONS

The statistical characteristics of the dataset used for surrogate model identification were first analysed to verify the independence and coverage of the sampled operating variables. The correlation heatmap (Figure 3) indicates weak pairwise correlations among inputs, minimising multicollinearity during training.

Figure 4 displays the LHS generated step durations for t_{pres}, t_{depres}, t_{ads}, t_{LR}, and t_{HR}. The plots show patterns consistent with stratified, quasi-independent draws. Note that the horizontal axis represents the sample order of LHS points, evidencing broad coverage of the operating domain for each step.

The analytical surrogate expressions obtained using the SR approach for predicting CO_2 purity and recovery are presented in Equations 6 and 7. The resulting symbolic forms represent compact yet accurate approximations of the nonlinear mappings between the process decision variables.

$$Pur_{CO_2} = \sin\left(\frac{t_{ads} + 0.058}{sin^3\left(\frac{1}{cos\left(t_{depres}^3\right)}\right) + sin\left(t_{depres} e^{cos(0.609)}\right)}\right) \tag{6}$$

$$Rec_{CO_2} = 0.91\cos^4\left(e^{-4(\sin(t_{depres}/0.94)\sin(t_{ads}))^2} t_{ads}\right) \quad (7)$$

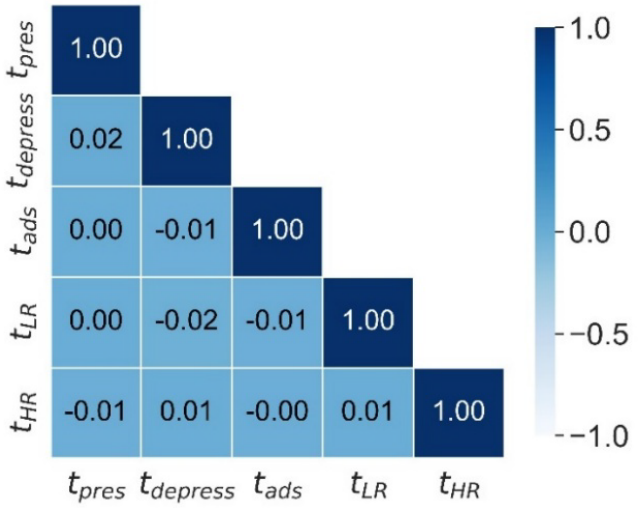

Figure 3. Correlation heatmap for the input variables of the surrogate models.

Both SR-derived equations capture the nonlinear dependence of CO_2 purity and recovery on the durations of the adsorption (t_{ads}) and depressurisation (t_{depres}) steps. Their explicit analytical structure facilitates low-complexity surrogate representation suitable for direct embedding into optimisation routines.

The DNN developed for predicting CO_2 purity used a fully connected feedforward architecture with five input features and four hidden layers, employing the ReLU activation function. The hidden layers comprised 300, 200, 50, and 200 neurons, respectively, followed by a single linear output neuron. This configuration resulted in 82451 trainable parameters. The model was trained using the Adam optimiser with a learning rate of 0.001 and MSE as the loss function.

Similarly, the DNN model designed for CO_2 recovery employed the same input structure and ReLU-activated hidden layers, but with a more compact topology. The network consisted of two hidden layers containing 300 and 100 neurons, respectively, also followed by a single linear output neuron. The total number of trainable parameters in this configuration was 32001. This model was also trained with the Adam optimiser at a learning rate of 0.001, ensuring consistent training dynamics and convergence across both networks.

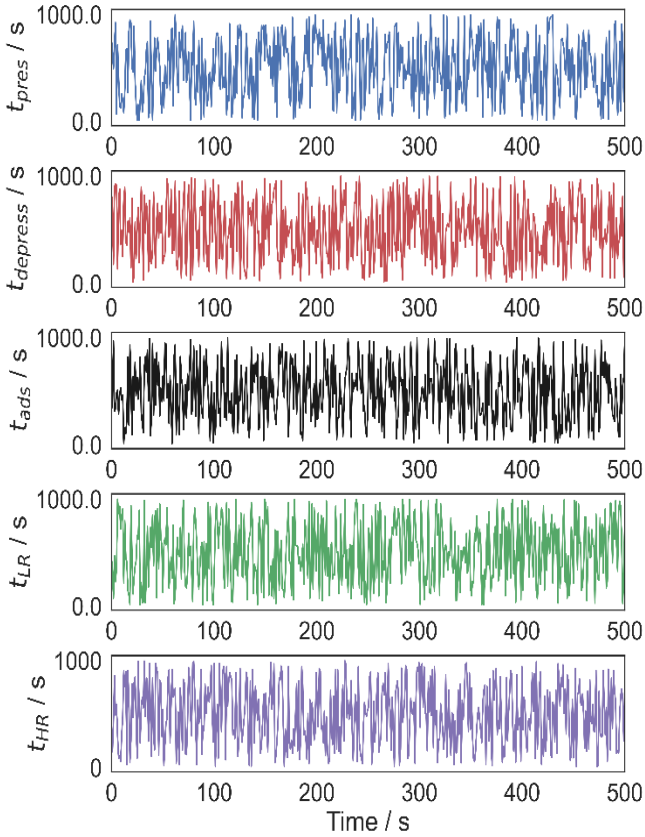

Figure 4. Sampled PSA Step Durations Generated by LHS.

Figure 5 compares the parity plots for the two surrogate modelling approaches used to predict CO_2 purity and recovery. Subfigures 5a and 5b correspond to the SR-based models, while subfigures 5c and 5d refer to the DNN surrogates. In all cases, the predicted values exhibit a good agreement with the reference data. The mechanistic PSA model has the points tightly distributed along the identity line. A slightly better predictive performance is observed for the DNN models, which exhibit lower dispersion and greater alignment along the diagonal, reflecting their enhanced capacity to capture complex nonlinear relationships.

Table 1 summarises the prediction errors obtained for both surrogate modelling strategies. The metrics considered were the MSE and MAE, both computed in the denormalised domain for direct physical interpretation. The DNN models outperform the SR surrogates in predictive accuracy, with MSE values one to two orders of magnitude lower. Nevertheless, the symbolic regression models also demonstrate satisfactory performance, achieving low error rates and accurately reproducing the PSA system's main nonlinear trends.

The multi-objective optimisation procedure was carried out using the PSO algorithm, configured with a swarm of 100 particles and 100 iterations. Both surrogate-based frameworks (SR and DNN models) were

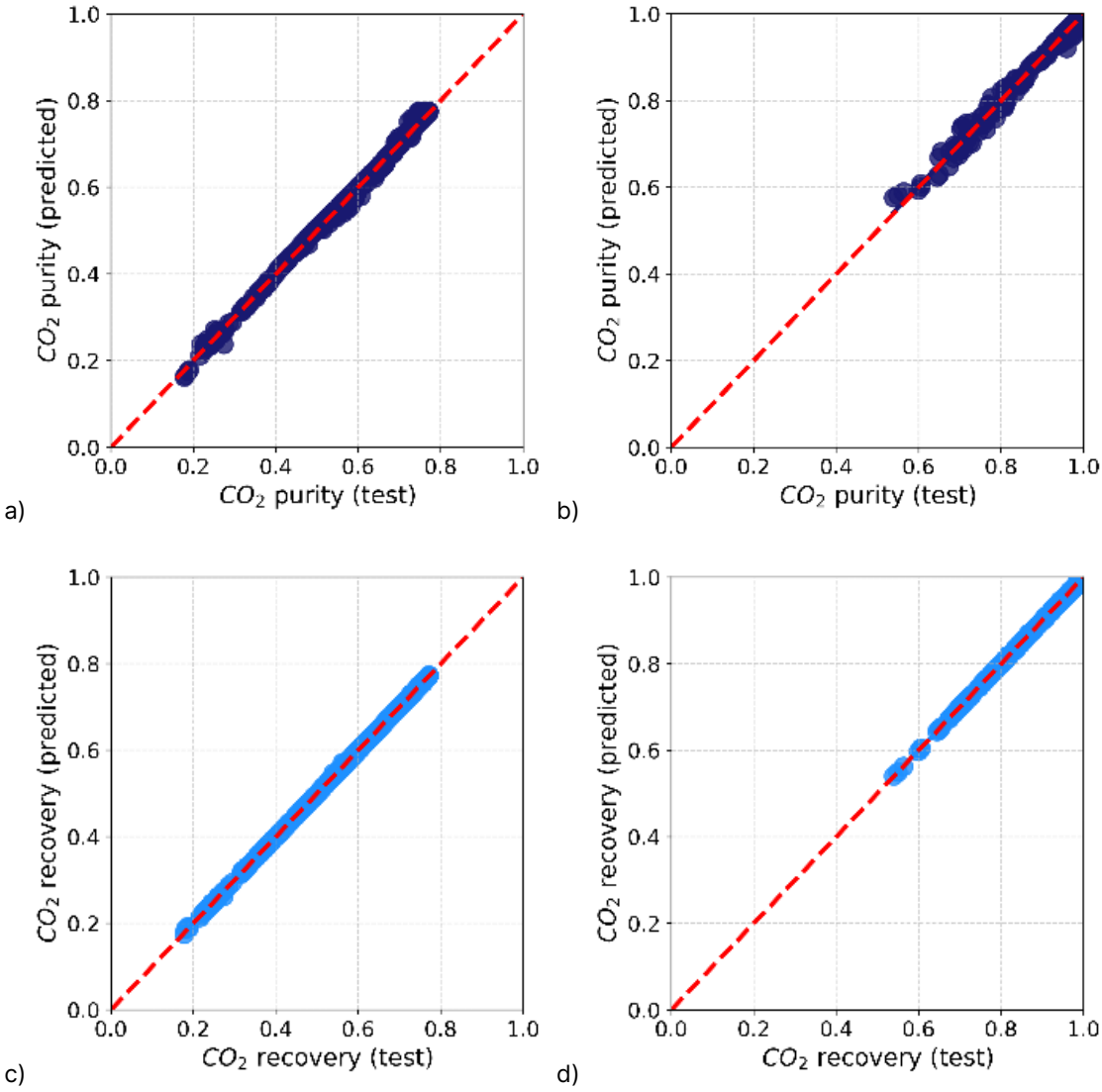

Figure 5. Parity plots comparing predicted and reference values for CO_2 purity and recovery obtained with SR (a, b) and DNN (c, d) surrogate models.

employed in the optimisation problem defined in Section 2. Additionally, the optimisation results were compared with those obtained using the mechanistic PSA model, which was optimised under the same conditions but with 50 particles and 50 iterations. The decision variable values corresponding to the Pareto-optimal points from each surrogate model were further evaluated in the mechanistic simulator to verify the consistency and physical plausibility of the predicted solutions. The resulting Pareto fronts, illustrated in Figure 6, display the trade-off between CO_2 purity and CO_2 recovery for each modelling strategy.

Table 1: Final MSE and MAE values for the test dataset obtained with the SR and DNN surrogate models.

Model	Variable	MSE	MAE
SR	CO_2 purity	5.0×10^{-5}	4.33×10^{-3}
SR	CO_2 recovery	5.9×10^{-5}	4.03×10^{-3}
DNN	CO_2 purity	1.24×10^{-6}	5.70×10^{-4}
DNN	CO_2 recovery	5.22×10^{-7}	5.11×10^{-4}

The optimisation using the SR surrogate produced a Pareto front containing 4345 optimal solutions, while the DNN surrogate yielded 508 points. Despite both optimisations using the same number of particles and iterations, the SR-based approach produced a denser, more diverse Pareto front, indicating superior exploration of the solution space compared to the DNN model.

This is attributed to the continuous and differentiable nature of the analytical expressions derived via SR,

which induces a smoother optimisation landscape, facilitating uniform exploration of the trade-off region by the PSO algorithm. In contrast, DNN surrogates may introduce local irregularities and discontinuities due to nonlinear activation functions such as ReLU, causing the swarm to concentrate on fewer regions of the Pareto front and resulting in a sparser front.

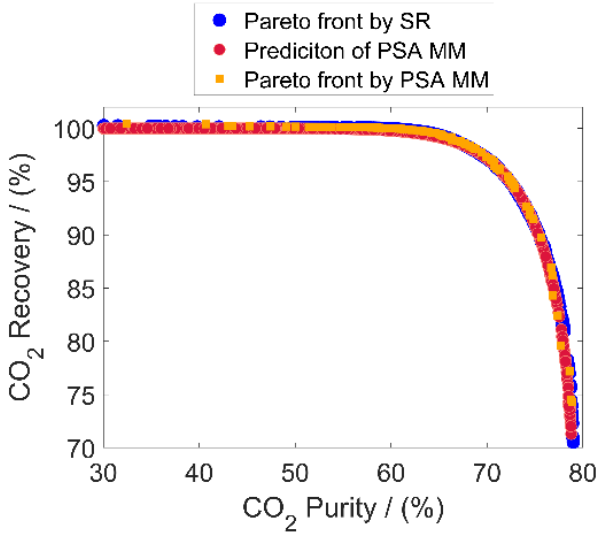

a) Pareto front by SR surrogate

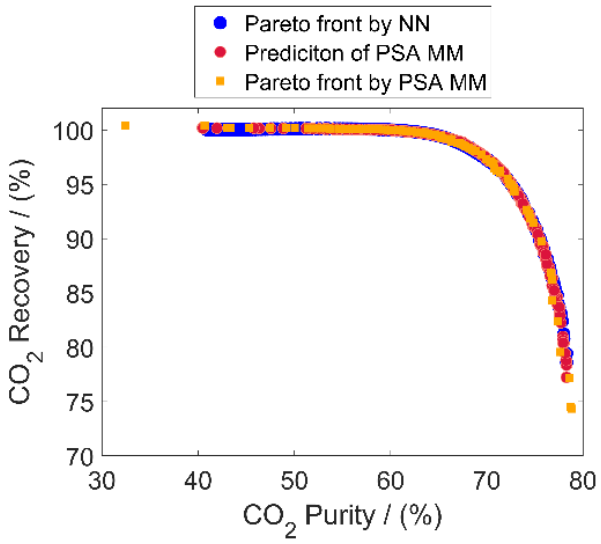

b) Pareto front by DNN surrogate.

Figure 6. Comparison of Pareto fronts obtained with SR and DNN surrogates against the PSA MM.

Figure 7 presents the cumulative optimisation time per iteration obtained for both surrogate-based optimisation frameworks. Each curve represents the total computation time accumulated across all particles up to a given PSO iteration. The SR-based optimisation required a total of 38.6 s to complete the 100 iterations, whereas the DNN-based framework required 1331.5 s under the same conditions.

These results highlight a substantial difference in computational efficiency: the SR approach was approximately 34.5 times faster than the DNN model. This performance gap arises mainly from the analytical nature of the SR surrogates, which allow direct function evaluations without the matrix operations and backpropagation overhead inherent to neural networks. Consequently, SR models enable a much faster exploration of the search space while maintaining sufficient predictive accuracy for the multiobjective optimisation task.

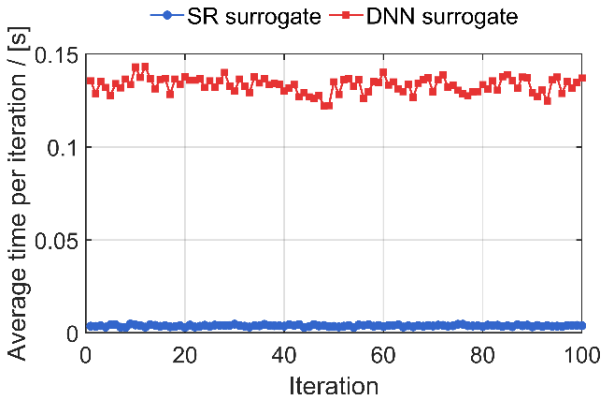

Figure 7. Average computational cost per iteration of optimisation using surrogate SR and DNN models.

CONCLUSION

This study demonstrated that SR can serve as an efficient surrogate modelling strategy for optimising PSA processes. Compared to DNN, the SR-based framework achieved faster convergence and produced a more diverse Pareto front while maintaining good predictive accuracy. These findings highlight the potential of SR as a computationally lightweight alternative for data-driven optimisation of cyclic adsorption systems, offering a balance between robustness, and efficiency.

ACKNOWLEDGEMENTS

The present work contributes to completion of a sub project at SUBPRO, a research-based innovation center within Subsea Production and Processing at the Norwe gian University of Science and Technology. The authors would like to express their gratitude for the financial support received from SUBPRO, funded by the Research Council of Norway through grant number 237893, major industry partners, and NTNU.

REFERENCES

1. Angelis D, Sofos F, Karakasidis TE. Artificial

intelligence in physical sciences: symbolic regression trends and perspectives. Arch Computat Methods Eng 30:3845-3865 (2023). https://doi.org/10.1007/s11831-023-09922-z
2. Capra, F., Gazzani, M., Joss, L., Mazzotti, M., and Martelli, E. (2018). MO-MCS, a derivative-free algorithm for the multiobjective optimisation of adsorption processes. Technical report.
3. Costa EA, Rebello CM, Schnitman L, Loureiro JM, Ribeiro AM, Nogueira IBR. Adaptive digital twin for pressure swing adsorption systems: integrating a novel feedback tracking system, online learning and uncertainty assessment for enhanced performance. Engineering Applications of Artificial Intelligence 127:107364 (2024). https://doi.org/10.1016/j.engappai.2023.107364
4. Cozad A, Sahinidis NV, Miller DC. Learning surrogate models for simulation?based optimization. AIChE Journal 60:2211-2227 (2014). https://doi.org/10.1002/aic.14418
5. De Witte N, Denayer JFM, Van Assche TRC. Effect of adsorption duration and purge flowrate on pressure swing adsorption performance. Ind. Eng. Chem. Res. 60:13684-13691 (2021). https://doi.org/10.1021/acs.iecr.1c02291
6. Ben-Mansour R, Habib MA, Bamidele OE, Basha M, Qasem NAA, Peedikakkal A, Laoui T, Ali M. Carbon capture by physical adsorption: materials, experimental investigations and numerical modeling and simulations – a review. Applied Energy 161:225-255 (2016). https://doi.org/10.1016/j.apenergy.2015.10.011
7. Hale WT, Safikou E, Bollas GM. Inference of faults through symbolic regression of system data. Computers & Chemical Engineering 157:107619 (2022). https://doi.org/10.1016/j.compchemeng.2021.107619
8. Hu W, Zhang L. First-principles, machine learning and symbolic regression modelling for organic molecule adsorption on two-dimensional cao surface. Journal of Molecular Graphics and Modelling 124:108530 (2023). https://doi.org/10.1016/j.jmgm.2023.108530
9. Kalman V, Voigt J, Jordan C, Harasek M. Hydrogen purification by pressure swing adsorption: high-pressure PSA performance in recovery from seasonal storage. Sustainability 14:14037 (2022). https://doi.org/10.3390/su142114037
10. Kamin Z, Bahrun MHV, Bono A. A short review on pressure swing adsorption (PSA) technology for nitrogen generation from air. AIP Conference Proceedings 2656:050006 (2022). https://doi.org/10.1063/5.0099702
11. Kay H, Kay S, Mowbray M, Lane A, Mendoza C, Martin P, Zhang D. Constructing a symbolic regression-based interpretable soft sensor for industrial data analytics and product quality control. Ind. Eng. Chem. Res. 63:4083-4092 (2024). https://doi.org/10.1021/acs.iecr.3c04021
12. Khajuria H, Pistikopoulos EN. Optimization and control of pressure swing adsorption processes under uncertainty. AIChE Journal 59:120-131 (2012). https://doi.org/10.1002/aic.13783
13. Leperi KT, Yancy-Caballero D, Snurr RQ, You F. 110th anniversary: surrogate models based on artificial neural networks to simulate and optimize pressure swing adsorption cycles for co₂ capture. Ind. Eng. Chem. Res. 58:18241-18252 (2019). https://doi.org/10.1021/acs.iecr.9b02383
14. Li, L., Jamieson, K., DeSalvo, G., Rostamizadeh, A., & Talwalkar, A. (2018). Hyperband: A novel bandit-based approach to hyperparameter optimization. *Journal of machine learning research*, *18*(185), 1-52.
15. Luberti M, Ahn H. Review of polybed pressure swing adsorption for hydrogen purification. International Journal of Hydrogen Energy 47:10911-10933 (2022). https://doi.org/10.1016/j.ijhydene.2022.01.147
16. Makke N, Chawla S. Interpretable scientific discovery with symbolic regression: a review. Artif Intell Rev 57: (2024). https://doi.org/10.1007/s10462-023-10622-0
17. Nikolaidis, G.N., Kikkinides, E.S., and Georgiadis, M.C. (2015). Modelling and simulation of pressure swing adsorption (psa) processes for post-combustion carbon dioxide (co2) capture from flue gas. In K.V. Gernaey, J.K. Huusom, and R. Gani (eds.), 12th.
18. International Symposium on Process Systems Engineering and 25th European Symposium on Computer Aided Process Engineering, volume 37 of Computer Aided Chemical Engineering, 287–292. Elsevier. doi: https://doi.org/10.1016/B978-0-444-63578-5.50043-8
19. Nikolaidis GN, Kikkinides ES, Georgiadis MC. Model-based approach for the evaluation of materials and processes for post-combustion carbon dioxide capture from flue gas by PSA/VSA processes. Ind. Eng. Chem. Res. 55:635-646 (2016). https://doi.org/10.1021/acs.iecr.5b02845
20. Nogueira IBR, Dias ROM, Rebello CM, Costa EA, Santana VV, Rodrigues AE, Ferreira A, Ribeiro AM. A novel nested loop optimization problem based on deep neural networks and feasible operation regions definition for simultaneous material screening and process optimization. Chemical Engineering Research and Design 180:243-253

(2022). https://doi.org/10.1016/j.cherd.2022.02.013
21. Panerati J, Schnellmann MA, Patience C, Beltrame G, Patience GS. Experimental methods in chemical engineering: artificial neural networks–anns. Can J Chem Eng 97:2372-2382 (2019). https://doi.org/10.1002/cjce.23507
22. Quade M, Abel M, Shafi K, Niven RK, Noack BR. Prediction of dynamical systems by symbolic regression. Phys. Rev. E 94: (2016). https://doi.org/10.1103/physreve.94.012214
23. Rebello CM, Costa EA, Fontana M, Schnitman L, Nogueira IBR. Interpretable scientific machine learning approach for correcting phenomenological models: methodology validation on an ESP prototype. Ind. Eng. Chem. Res. 63:19030-19050 (2024). https://doi.org/10.1021/acs.iecr.4c02104
24. Rebello CM, Nogueira IBR. Optimizing 2 capture in pressure swing adsorption units: a deep neural network approach with optimality evaluation and operating maps for decision-making. Separation and Purification Technology 340:126811 (2024). https://doi.org/10.1016/j.seppur.2024.126811
25. Scheffold L, Finkler T, Piechottka U. Gray-box system modeling using symbolic regression and nonlinear model predictive control of a semibatch polymerization. Computers & Chemical Engineering 146:107204 (2021). https://doi.org/10.1016/j.compchemeng.2020.107204
26. Subraveti SG, Li Z, Prasad V, Rajendran A. Machine learning-based multiobjective optimization of pressure swing adsorption. Ind. Eng. Chem. Res. 58:20412-20422 (2019). https://doi.org/10.1021/acs.iecr.9b04173
27. Sofronova E, Diveev A. Universal approach to solution of optimization problems by symbolic regression. Applied Sciences 11:5081 (2021). https://doi.org/10.3390/app11115081
28. Tian T, Wang Y, Liu B, Ding Z, Xu X, Shi M, Ma J, Zhang Y, Zhang D. Simulation and experiment of six-bed PSA process for air separation with rotating distribution valve. Chinese Journal of Chemical Engineering 42:329-337 (2022). https://doi.org/10.1016/j.cjche.2021.03.027
29. Tonda A. Review of pysr: high-performance symbolic regression in python and julia. Genet Program Evolvable Mach 26: (2024). https://doi.org/10.1007/s10710-024-09503-4
30. Ward A, Pini R. Efficient bayesian optimization of industrial-scale pressure-vacuum swing adsorption processes for co₂ capture. Ind. Eng. Chem. Res. 61:13650-13668 (2022). https://doi.org/10.1021/acs.iecr.2c02313
31. Zhang R, Shen Y, Tang Z, Li W, Zhang D. A review of numerical research on the pressure swing adsorption process. Processes 10:812 (2022). https://doi.org/10.3390/pr10050812